

## Mean, Variability, and Trend of Southern Ocean Wind Stress: Role of Wind Fluctuations

XIA LIN

*Polar Climate System and Global Change Laboratory, Nanjing University of Information Science and Technology, Nanjing, China, and Centre for Ocean and Atmospheric Sciences, School of Environmental Sciences, University of East Anglia, Norwich, United Kingdom*

XIAOMING ZHAI

*Centre for Ocean and Atmospheric Sciences, School of Environmental Sciences, University of East Anglia, Norwich, United Kingdom*

ZHAOMIN WANG

*College of Oceanography, Hohai University, Nanjing, China*

DAVID R. MUNDAY

*British Antarctic Survey, Cambridge, United Kingdom*

(Manuscript received 19 July 2017, in final form 30 January 2018)

### ABSTRACT

The Southern Ocean (SO) surface westerly wind stress plays a fundamental role in driving the Antarctic Circumpolar Current and the global meridional overturning circulation. Here, the authors investigate the contributions of atmospheric wind fluctuations to the mean, variability, and trend of SO wind stress over the last four decades using NCEP reanalysis and ERA-Interim products. Including wind variability at synoptic frequencies (2–8 days) and higher in the stress calculation is found to increase the strength of the mean SO wind stress by almost 40% in both reanalysis products. The southern annular mode index is found to be a good indicator for the strength of the mean wind and mean wind stress, but not as good an indicator for wind fluctuations, at least for the chosen study period. Large discrepancies between reanalysis products emerge regarding the contributions of wind fluctuations to the strengthening trend of SO wind stress. Between one-third and one-half of the stress trend in NCEP can be explained by the increase in the intensity of wind fluctuations, while the stress trend in ERA-Interim is due entirely to the increasing strength of the mean westerly wind. This trend discrepancy may have important climatic implications since the sensitivity of SO circulation to wind stress changes depends strongly on how these stress changes are brought about. Given the important role of wind fluctuations in shaping the SO wind stress, studies of the SO response to wind stress changes need to account for changes of wind fluctuations in the past and future.

### 1. Introduction

The Southern Hemisphere (SH) surface westerly wind stress is a major forcing for driving the Antarctic Circumpolar Current (ACC) and upwelling of deep waters in the Southern Ocean (SO). The SH westerly wind stress has strengthened significantly over the last few decades and is projected to continue to do so in the

future, which may have important implications for the global climate system via modulating the rate at which the SO uptakes heat and carbon (e.g., [Thompson and Solomon 2002](#); [Le Quéré et al. 2007](#); [Marshall and Speer 2012](#); [Wang et al. 2015, 2017](#)). The strength of the SO wind stress is found to be closely related to the phase of the southern annular mode (SAM), the dominant mode of atmospheric variability in the SH, with wind stress being stronger (and also poleward shifted) during the positive phase of the SAM (e.g., [Marshall 2003](#); [Swart and Fyfe 2012](#)). However, the SAM index is often

---

*Corresponding author:* Xiaoming Zhai, [xiaoming.zhai@uea.ac.uk](mailto:xiaoming.zhai@uea.ac.uk)

defined based on the monthly, seasonal-, or annual-mean zonal sea level pressure difference between 40° and 65°S (Gong and Wang 1999), and as such is a measure of the monthly-, seasonal-, or annual-mean strength of the westerly winds, rather than westerly wind stress. This could be problematic, since it is well known that the surface wind stress depends nonlinearly on surface wind velocity (e.g., Large et al. 1994; Zhai et al. 2012).

Because of the aforementioned nonlinear dependence of wind stress on surface wind, high-frequency wind fluctuations contribute to wind stress variability at both high and low frequencies (Zhai et al. 2012; Zhai 2013). For example, including wind fluctuations with time scales less than 1 month in the wind stress calculation significantly enhances the strength of the time-mean and seasonal-mean wind stress, particularly at mid- and high latitudes. In turn, this increases wind power input to the ocean general circulation by over 70% (Zhai et al. 2012; Wu et al. 2016). Therefore, studies on the changes of SO wind stress and their impact on the ocean need to take into account changes of not only the low-frequency (e.g., interannual) variability of the westerly jet, but also wind fluctuations at much shorter time scales (e.g., days).

The strong positive trend of SO wind stress seen in observations, as well as atmospheric reanalysis products, has spurred a great deal of interest in how the SO responds to changes of surface wind stress forcing (e.g., Hallberg and Gnanadesikan 2001, 2006; Meredith and Hogg 2006; Böning et al. 2008; Farneti et al. 2010; Dufour et al. 2012; Munday et al. 2013; Bishop et al. 2016). This includes a number of steady-state sensitivity modeling studies where the mean SO wind stress is strengthened and/or shifted (e.g., Downes et al. 2011; Zhai and Munday 2014; Spence et al. 2014; Munday and Zhai 2015; Bishop et al. 2016; Hogg et al. 2017), as well as some observational and modeling studies of the transient response of the ACC and SO eddy field to changes of the SAM (e.g., Meredith and Hogg 2006; Screen et al. 2009; O’Kane et al. 2013; Langlais et al. 2015). Two dynamical phenomena—eddy saturation (Straub 1993) and eddy compensation (Viebahn and Eden 2010), which refer to the loss and reduced sensitivity of ACC transport and SO meridional overturning circulation to wind stress changes, respectively—emerge from model studies with resolved or permitted, rather than parameterized, mesoscale ocean eddies.<sup>1</sup> Model investigations into the eddy saturation and eddy compensation phenomena typically involve directly varying the

magnitude of the mean wind stress in the SO. The underlying assumption of this approach is that the stress varies due to changes of the mean wind.<sup>2</sup> In reality, however, some of the observed and predicted wind stress changes may be brought about by changes in the variability of the atmospheric wind, owing to the nonlinear nature of the stress law (Zhai 2013).

An exception to this common practice of directly varying the mean wind stress is a recent study by Munday and Zhai (2017), who investigated the impact of wind fluctuations on the sensitivity of SO stratification and circulation to wind stress changes. In their study, changes of the mean wind stress felt by the ocean were made through alteration of the wind variability, as opposed to the mean wind. Stronger wind variability is found to enhance near-surface energy dissipation and increase near-surface viscous and diffusive mixing (see also Jouanno et al. 2016; Sinha and Abernathy 2016). The increased vertical mixing deepens the surface mixed layer and results in a much greater sensitivity (more than doubled) of the SO meridional overturning circulation to the increased wind stress, when compared to equivalent experiments forced by changing the mean wind. This result has important implications for understanding the SO response to past and future wind stress changes, should changes in wind stress be brought about not only by changes of the mean wind, but also by changes of wind variability. However, to our knowledge, there have been few studies (Zhai et al. 2012; Zhai 2013; Franzke et al. 2015) so far assessing the role of wind fluctuations in determining the mean, variability, and trend of the observed wind stress in the SO. A number of studies exist on the changes of the SH storm track and cyclone activities (Simmonds and Keay 2000; Yin 2005; Grieger et al. 2014; Wang et al. 2016; Chang 2017). However, the link between changes in these synoptic atmospheric systems and changes in SO wind stress has not yet been made.

In this study, we use reanalysis data products to investigate the contributions of wind fluctuations on different time scales (6 h–2 days, 2–8 days, and 8 days–1 yr) to the mean, variability, and trend of SO wind stress for the first time. The paper is organized as follows. We begin in section 2 by describing the reanalysis products and analysis methods used in this study. In section 3, we first examine the effect of wind fluctuations on the time-mean and seasonal-mean wind stresses in the SO, and

<sup>1</sup> Non-eddy-resolving ocean models with a variable eddy parameterization coefficient are found to be capable of achieving partial eddy compensation (e.g., Farneti et al. 2010; Gent 2016).

<sup>2</sup> If the increase in the magnitude of the mean wind stress is a result of increased wind variability, there should be a concurrent increase in wind stress variability, but this is absent in sensitivity model experiments where the strength of the mean stress is directly varied (e.g., doubled). High-frequency wind stress fluctuations are known to be important in setting the surface mixed layer depth (e.g., Zhou et al. 2018).

this is followed by an investigation of the contribution of wind fluctuations to wind stress differences between positive and negative SAM years, as well as their contribution to the observed strengthening trend of SO wind stress. Finally, section 4 provides a summary and some concluding remarks.

## 2. Data and methods

### a. Reanalysis data

Six-hourly, 10-m wind fields from two widely used atmospheric reanalysis products are analyzed in this study: National Centers for Environmental Prediction (NCEP)–National Center for Atmospheric Research (NCAR) reanalysis (NCEP-1; Kalnay et al. 1996) and the European Centre for Medium-Range Weather Forecasts (ECMWF) interim reanalysis (ERA-Interim; Dee et al. 2011). The NCEP-1 and ERA-Interim 10-m winds are provided on spectral T62 (~210 km) and T255 (~80 km) grids, respectively. Prior to 1979, the strength of the SH westerly jet in the NCEP-1 reanalysis product shows large spurious trends when compared to that derived from station data, owing to the gradual reduction of errors in the NCEP-simulated sea level pressure field at high southern latitudes (Hines et al. 2000; Marshall 2003). The situation is much improved with the introduction of the Television Infrared Observation Satellite (TIROS) Operational Vertical Sounder data into the reanalysis assimilation scheme after 1979. Because of this, we choose the analysis period in this study to be from January 1979 to December 2016. Previous studies find that although ERA-Interim is somewhat better in representing the characteristics of extratropical cyclones than NCEP-1 due to its higher spatial resolution (e.g., Jung et al. 2006; Tilinina et al. 2013), both reanalysis products tend to underestimate the dynamical intensity (e.g., maximum wind speed) of mesoscale atmospheric features, such as mesocyclones and polar lows (Zappa et al. 2014; Verezemskaya et al. 2017). Figure 1 shows the comparison between the reanalysis winds and observed winds at four automatic weather stations from the Scientific Committee on Antarctic Research (SCAR) Reference Antarctic Data for Environmental Research (READER) project (Turner et al. 2004). The two reanalysis products reproduce reasonably well the salient features of wind variability at the four locations, but they both underestimate the amplitude of wind variability, most notably at high frequencies (e.g., 6 h–2 days). Therefore, results from our study should be considered as a lower bound of the contribution of wind fluctuations to the SO wind stress, particularly at high frequencies.

The NCEP–DOE reanalysis product (NCEP-2; Kanamitsu et al. 2002), an improved version of NCEP-1,<sup>3</sup> and the Japanese 55-year Reanalysis product (JRA-55; Kobayashi et al. 2015) provided on the spectral T319 (~63 km) grid are also analyzed in this study. Since the results from NCEP-2 and JRA-55 are very similar to those from NCEP-1 and ERA-Interim, except for the trend, we only include results from NCEP-2 and JRA-55 when comparing trends of SO wind stress among different reanalysis products.

### b. SAM index

Here, we use the station-based SAM index data from Marshall (2003; updated online). The SAM index is defined, following Gong and Wang (1999), as

$$\text{SAM} = P_{40^{\circ}\text{S}}^* - P_{65^{\circ}\text{S}}^*,$$

where  $P_{40^{\circ}\text{S}}^*$  and  $P_{65^{\circ}\text{S}}^*$  are the normalized monthly zonal-mean sea level pressure at 40° and 65°S, respectively, obtained by averaging records from six stations at roughly 65°S and six stations at roughly 40°S. Readers are referred to Marshall (2003) for the locations of these stations, as well as the criteria for choosing them. Note that the SAM indices derived from NCEP reanalysis and ERA-Interim products are found to be in very good agreement with that derived from station data after 1979 (Thompson and Solomon 2002; Marshall 2003).

### c. Wind stress

The zonal surface wind stress is calculated based on the bulk formula (Large et al. 1994)

$$\tau_x = \rho_a c_d |U_{10}| u_{10},$$

where  $\tau_x$  is the surface zonal wind stress,  $u_{10}$  is the 6-hourly 10-m zonal wind velocity,  $|U_{10}|$  is the 6-hourly 10-m wind speed from reanalysis data,  $\rho_a = 1.223 \text{ kg m}^{-3}$  is air density at the sea surface, and  $c_d$  is the drag coefficient with  $10^3 c_d = (2.7/|U_{10}|) + 0.142 + 0.0764|U_{10}|$ . Here, we do not explicitly investigate the role of the variable drag coefficient, although its effect is included in the wind stress calculations. Ocean surface velocity is not considered here in the stress calculation since its effect on the magnitude of SO wind stress is very small (a few percentages at most; see Wu et al. 2017). The zonal wind stress calculated from the bulk formula is slightly weaker than that provided in the reanalysis products, owing to additional adjustments applied in the reanalysis models (W. Ebisuzali 2017, NOAA, personal communication).

<sup>3</sup>The improvements include an updated model with better physical parameterizations and fixing known data assimilation errors in NCEP-1.

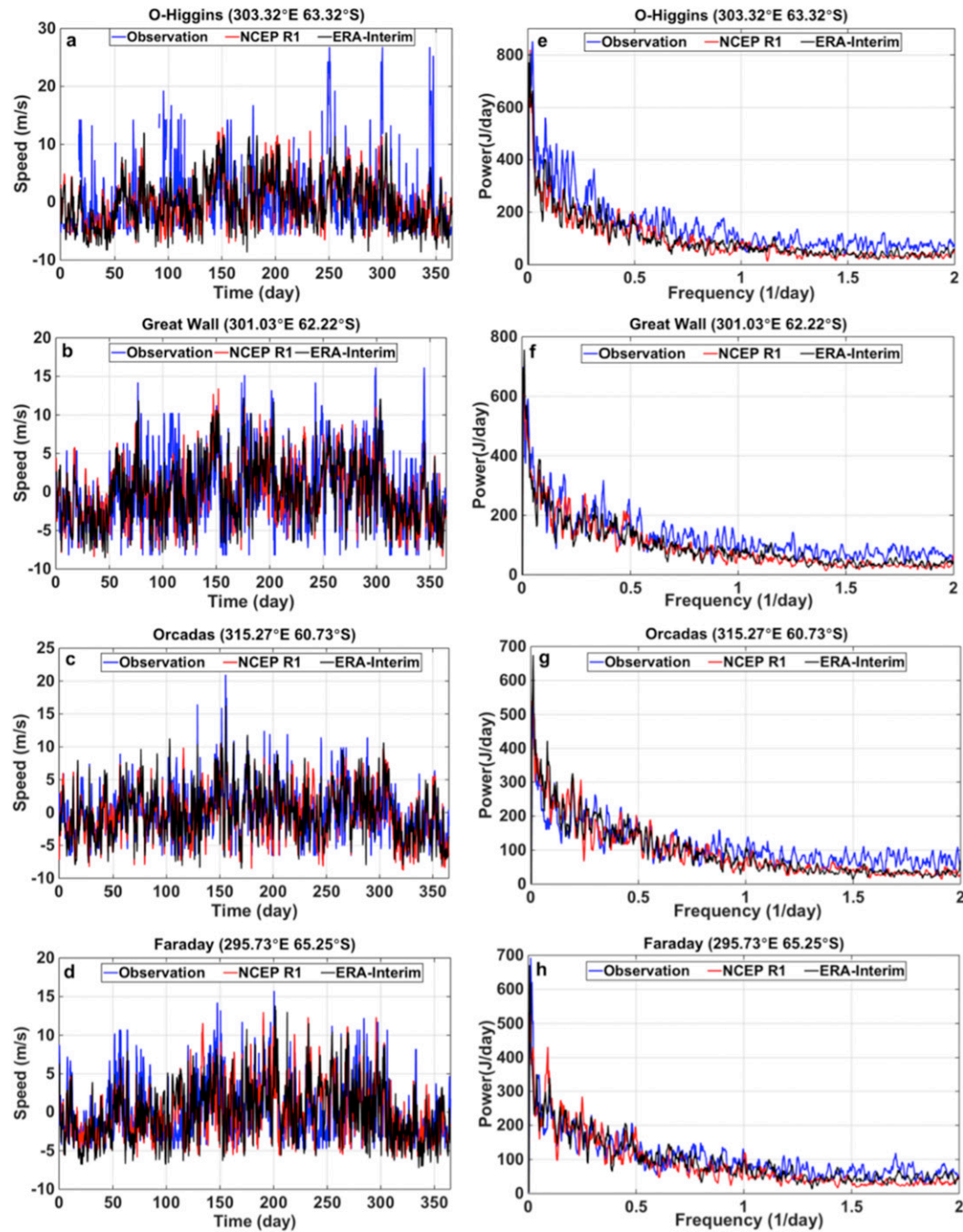


FIG. 1. Comparison of the time series and power spectra of 10-m wind speeds from NCEP-1 and ERA-Interim with automatic weather station data at four locations in 1989 (with the annual mean removed). The wind speeds are observed at 10, 10, 6, and 11 m at O'Higgins, Great Wall, Orcadas, and Faraday, respectively.

To quantify the effect of wind fluctuations on different time scales on the SO wind stress, we apply 2-day running mean, 8-day running mean, and annual-mean averaging to the original 6-hourly reanalysis wind field to filter out wind fluctuations that last less than 2 days, less than 8 days, and less than 1 year, respectively. Threshold time scales of 2 and 8 days are chosen here because atmospheric variability

(e.g., wind and air temperature) on time scales of 2–8 days is generally thought to be associated with synoptic weather systems and baroclinic storm activities (e.g., Trenberth 1991; Inatsu and Hoskins 2004; Yin 2005). Figure 2 shows the magnitude of peak zonal-mean zonal wind stress in the SO as a function of the running mean time scale. The magnitude of peak zonal-mean zonal wind stresses in both

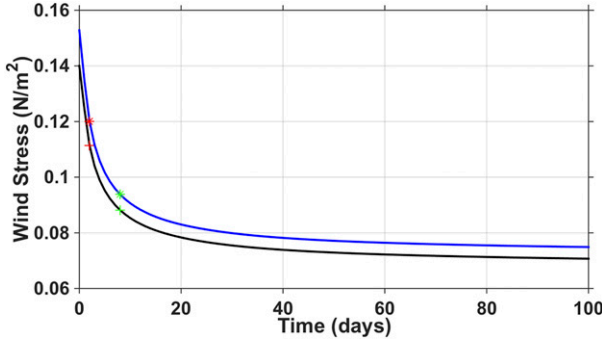


FIG. 2. The magnitude of peak zonal-mean zonal wind stress in the SO ( $35^{\circ}$ – $65^{\circ}$ S) averaged over 1979–2016 as a function of the running mean time scale from NCEP-1 (black line) and ERA-Interim (blue line). Red and green crosses (asterisks) mark peak zonal-mean zonal wind stresses calculated from NCEP-1 (ERA-Interim) 2- and 8-day running mean winds, respectively.

NCEP-1 and ERA-Interim decreases rapidly with increasing running mean time scale up to synoptic time scales ( $\sim 8$  days) and then decreases much more gently afterward. For example, increasing the running mean time scale to 10 or 15 days leads to only a 3% or 8% decrease in the calculated wind stresses, compared to those calculated from the 8-day running mean winds. Wind fluctuations on time scales of 2–8 days are calculated by taking the difference between the 2-day running mean and 8-day running mean wind fields. The 2–8-day filtered winds are then obtained by removing wind fluctuations on 2–8 days from the original 6-hourly wind field (Table 1). We recalculate the zonal

wind stresses using these filtered winds ( $\tau_{2d}$ ,  $\tau_{8d}$ ,  $\tau_{2-8d}$ , and  $\tau_{yr}$  from 2-day mean, 8-day mean, 2–8-day filtered, and annual-mean winds, respectively) and compare them with the zonal wind stress calculated from the 6-hourly reanalysis winds ( $\tau_{6hr}$ ). For example, since wind fluctuations on 6 h–2 days are excluded in the calculation of  $\tau_{2d}$ , the difference between  $\tau_{6hr}$  and  $\tau_{2d}$  can then be used to quantify the effect of including wind fluctuations on 6 h–2 days on the mean stress and its variability.

In addition to surface wind stress calculations, we also quantify kinetic energy of the wind field to help interpret some of the results shown in section 3. Mean kinetic energy in each year ( $MKE_{yr}$ ) is calculated from the annual-mean wind field, and eddy kinetic energy is calculated from wind fluctuations on time scales of 6 h–2 days ( $EKE_{2d}$ ), 2–8 days ( $EKE_{2-8d}$ ), 6 h–8 days ( $EKE_{8d}$ ), and 6 h–1 yr ( $EKE_{yr}$ ), respectively (see Table 1 for the formulas). For example,  $EKE_{2d}$  is calculated using the difference between the 6-hourly and 2-day running mean wind fields. As such,  $EKE_{2d}$  represents kinetic energy associated with wind fluctuations on time scales of 6 h–2 days alone and does not include the nonlinear cross term between fluctuations on 6 h–2 days and those on 2 days–1 yr.

### 3. Results

#### a. Mean

We first assess the effect of including wind fluctuations on different time scales on the mean wind stress in the

TABLE 1. List of variables and the formulas used to calculate them. Overbars  ${}^{-yr}$ ,  ${}^{-2d}$ ,  ${}^{-8d}$ , and  ${}^{-2-8d}$  represent annual mean, 2-day running mean, 8-day running mean, and 2–8-day filtered, respectively, and superscript “6hr” indicates 6-hourly reanalysis winds. The 2–8-day filtered winds ( $\bar{u}_{10}{}^{-2-8d}$  and  $\bar{v}_{10}{}^{-2-8d}$ ) are obtained by removing winds fluctuations on time scales of 2–8 days from the original 6-hourly reanalysis wind field and are calculated using  $\bar{u}_{10}{}^{-2-8d} = \bar{u}_{10}{}^{6hr} - (\bar{u}_{10}{}^{-2d} - \bar{u}_{10}{}^{-8d})$  and  $\bar{v}_{10}{}^{-2-8d} = \bar{v}_{10}{}^{6hr} - (\bar{v}_{10}{}^{-2d} - \bar{v}_{10}{}^{-8d})$ , respectively. The 2–8-day filtered wind speed ( $|\bar{U}_{10}{}^{-2-8d}|$ ) is then calculated from  $|\bar{U}_{10}{}^{-2-8d}| = \sqrt{(\bar{u}_{10}{}^{-2-8d})^2 + (\bar{v}_{10}{}^{-2-8d})^2}$ .

Variable	Definition	Formula
$\tau_{6hr}$	Zonal wind stress calculated from 6-hourly winds.	$\rho_a c_d  \bar{U}_{10}{}^{6hr}  \bar{u}_{10}{}^{6hr}$
$\tau_{2d}$	Zonal wind stress calculated from 2-day running mean winds.	$\rho_a c_d  \bar{U}_{10}{}^{-2d}  \bar{u}_{10}{}^{-2d}$
$\tau_{8d}$	Zonal wind stress calculated from 8-day running mean winds.	$\rho_a c_d  \bar{U}_{10}{}^{-8d}  \bar{u}_{10}{}^{-8d}$
$\tau_{2-8d}$	Zonal wind stress calculated from 2–8-day filtered winds.	$\rho_a c_d  \bar{U}_{10}{}^{-2-8d}  \bar{u}_{10}{}^{-2-8d}$
$\tau_{yr}$	Zonal wind stress calculated from annual-mean winds.	$\rho_a c_d  \bar{U}_{10}{}^{-yr}  \bar{u}_{10}{}^{-yr}$
$MKE_{yr}$	Kinetic energy associated with annual-mean winds.	$\frac{(\bar{u}_{10}{}^{-yr})^2 + (\bar{v}_{10}{}^{-yr})^2}{2}$
$EKE_{yr}$	Kinetic energy associated with wind fluctuations on time scales of 6 h–1 yr.	$\frac{(\bar{u}_{10}{}^{6hr} - \bar{u}_{10}{}^{-yr})^2 + (\bar{v}_{10}{}^{6hr} - \bar{v}_{10}{}^{-yr})^2}{2}$
$EKE_{2d}$	Kinetic energy calculated from wind fluctuations on time scales of 6 h–2 days alone.	$\frac{(\bar{u}_{10}{}^{6hr} - \bar{u}_{10}{}^{-2d})^2 + (\bar{v}_{10}{}^{6hr} - \bar{v}_{10}{}^{-2d})^2}{2}$
$EKE_{8d}$	Kinetic energy calculated from wind fluctuations on time scales of 6 h–8 days alone.	$\frac{(\bar{u}_{10}{}^{6hr} - \bar{u}_{10}{}^{-8d})^2 + (\bar{v}_{10}{}^{6hr} - \bar{v}_{10}{}^{-8d})^2}{2}$
$EKE_{2-8d}$	Kinetic energy calculated from wind fluctuations on time scales of 2–8 days alone.	$\frac{(\bar{u}_{10}{}^{-2d} - \bar{u}_{10}{}^{-8d})^2 + (\bar{v}_{10}{}^{-2d} - \bar{v}_{10}{}^{-8d})^2}{2}$

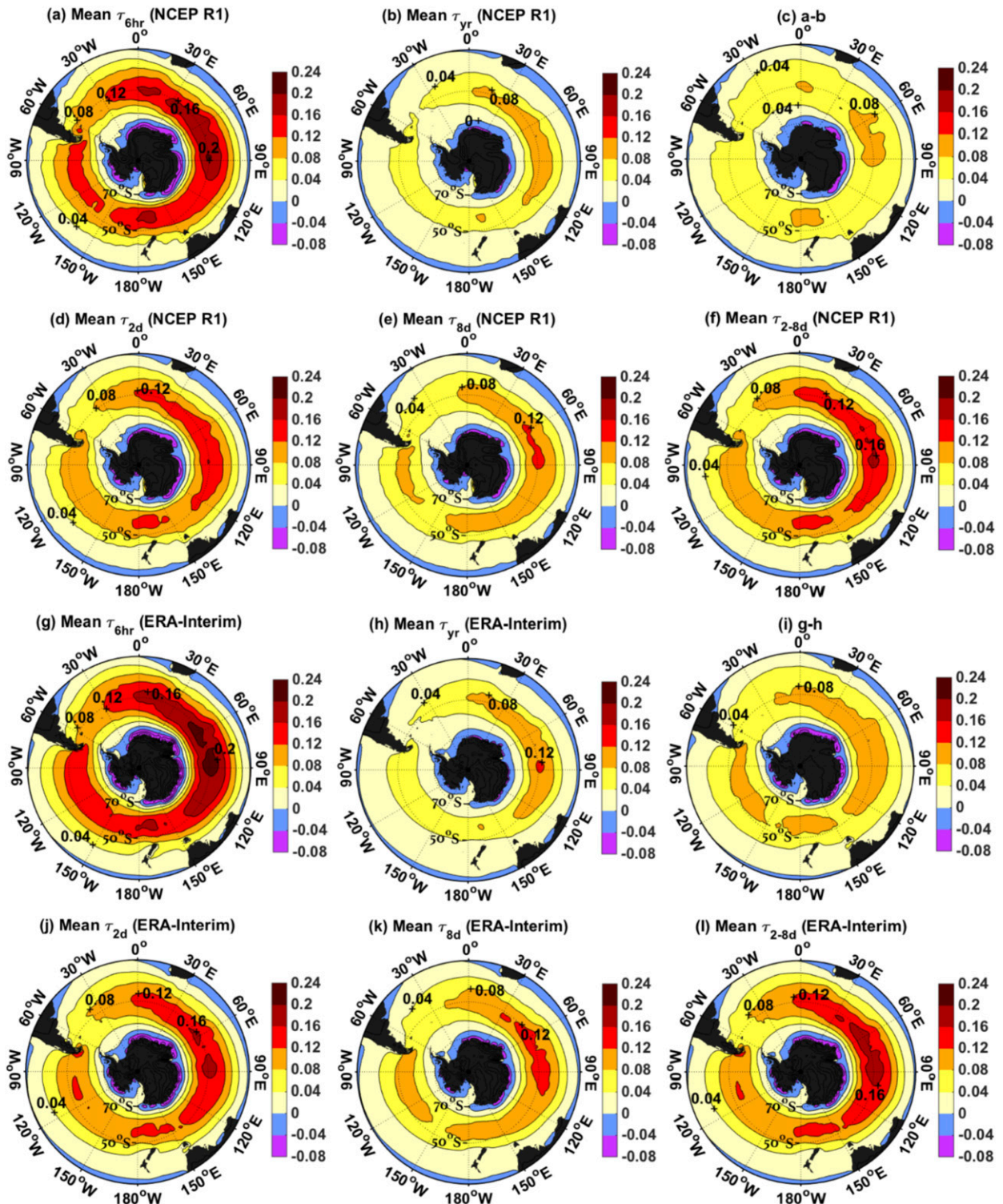


FIG. 3. The 1979–2016 time-mean wind stress ( $\text{N m}^{-2}$ ) in the SO from (a)–(f) NCEP-1 and (g)–(l) ERA-Interim. Mean  $\tau_{6\text{hr}}$ ,  $\tau_{2\text{d}}$ ,  $\tau_{8\text{d}}$ ,  $\tau_{2-8\text{d}}$ , and  $\tau_{\text{yr}}$  are calculated from 6-hourly, 2-day running mean, 8-day running mean, 2–8-day filtered, and annual-mean winds, respectively (see Table 1). (c),(i) Differences between  $\tau_{6\text{hr}}$  and  $\tau_{\text{yr}}$ , that is, (a) minus (b) and (g) minus (h), respectively.

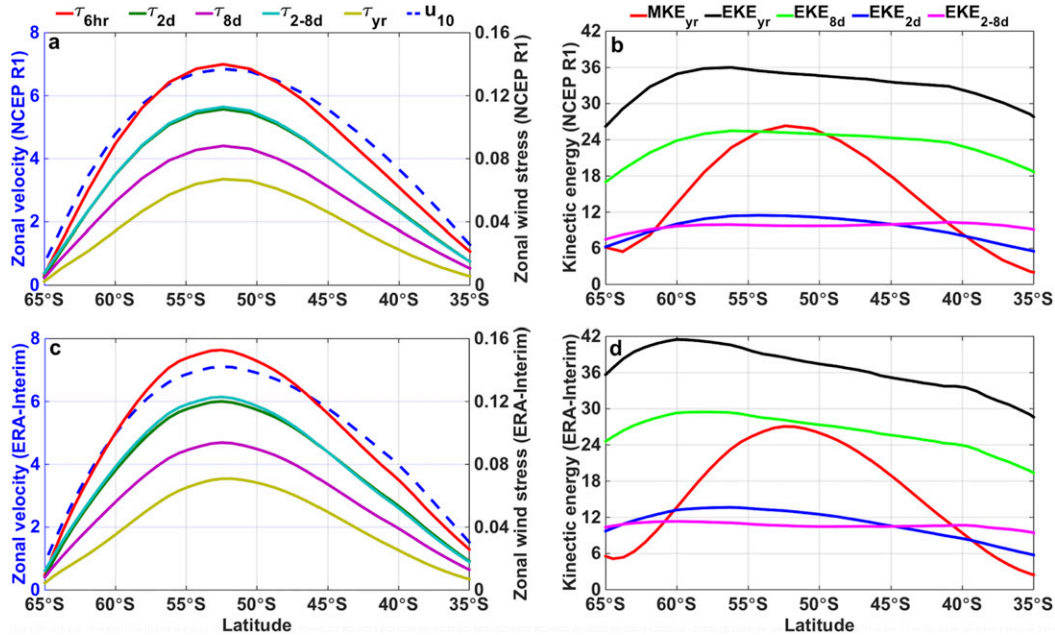


FIG. 4. The 1979–2016 zonal-mean and time-mean zonal wind velocity (dashed;  $\text{m s}^{-1}$ ), zonal wind stresses (solid;  $\text{N m}^{-2}$ ), and MKE and EKE ( $\text{m}^2 \text{s}^{-2}$ ) from (a),(b) NCEP-1 and (c),(d) ERA-Interim.  $\text{MKE}_{\text{yr}}$  is kinetic energy associated with the annual-mean winds, and  $\text{EKE}_{2\text{d}}$ ,  $\text{EKE}_{2-8\text{d}}$ ,  $\text{EKE}_{8\text{d}}$ , and  $\text{EKE}_{\text{yr}}$  are kinetic energy calculated from wind fluctuations on time scales of 6 h–2 days, 2–8 days, 6 h–8 days, and 6 h–1 yr, respectively (see Table 1).

SO. Figure 3 shows the 1979–2016 time-mean zonal wind stress calculated from the NCEP-1 (Figs. 3a–f) and ERA-Interim (Figs. 3g–l) reanalysis winds. Wind fluctuations are found to strengthen the mean wind stress almost everywhere in both reanalysis products, with the difference between multiyear mean  $\tau_{6\text{hr}}$  and  $\tau_{\text{yr}}$  often greater than  $\tau_{\text{yr}}$  itself (Figs. 3a–c and 3g–i). This indicates that the annual-mean wind alone can only explain roughly one-half of the annual-mean wind stress. The significant contribution of wind fluctuations to the mean SO wind stress is a result of the large wind variability in this storm-track region (Zhai 2013). Furthermore, the effect of including fluctuations on 6 h–8 days (Fig. 3a vs Fig. 3e; Fig. 3g vs Fig. 3k) is much larger than that of including fluctuations on 8 days–1 yr (Fig. 3e vs Fig. 3b; Fig. 3k vs Fig. 3h). Therefore, wind fluctuations on 6 h–8 days make a disproportionately large contribution to the mean stress. Quantitatively, including wind fluctuations in the stress calculation is found to increase the magnitude of peak zonal-mean wind stresses in NCEP-1 by about 109% (red vs yellow lines in Fig. 4a) and that in ERA-Interim by about 116% (Fig. 4c), with over 70% of both increases being contributed by wind fluctuations on 6 h–8 days (red vs purple lines in Figs. 4a,c). Including fluctuations on 6 h–2 days and those on 2–8 days appears to have a similar effect on the mean stress (overlapping green and cyan

lines in Figs. 4a,c), with both acting to strengthen the peak mean wind stress by roughly 20%.

To understand the effect of including wind fluctuations on different time scales on the mean wind stress, it is instructive to examine the magnitude and spatial structure of the MKE and EKE. Figure 5 shows the time-mean zonal wind velocity, MKE, and EKE calculated from wind fluctuations on different time scales from NCEP-1 (Figs. 5a–f) and ERA-Interim (Figs. 5g–l). The spatial patterns of the mean winds (Figs. 5a,g) are very similar to those of the mean wind stresses (Figs. 3a,g), with large values located in the south Indian Ocean sector. This similarity is also found in the zonal-mean patterns of the mean wind and mean stress (solid red and dashed blue lines in Figs. 4a,c), with the peak values of both quantities found at  $52^{\circ}$ – $53^{\circ}\text{S}$ . Another striking feature in Fig. 5 is the much broader and more uniform meridional (and zonal) distribution of the EKE, compared to the MKE (Figs. 5b,c,h,i). The zonal-mean EKE increases gradually southward in the latitude band of  $40^{\circ}$ – $60^{\circ}\text{S}$  and experiences somewhat sharper drops only north of  $\sim 40^{\circ}\text{S}$  and south of  $\sim 60^{\circ}\text{S}$  (Figs. 4b,d). This more-or-less uniform distribution of the EKE explains why the mean wind and mean stress peak at the same latitude: the strengthening of the mean stress owing to wind variability is largest where the mean wind is strongest.

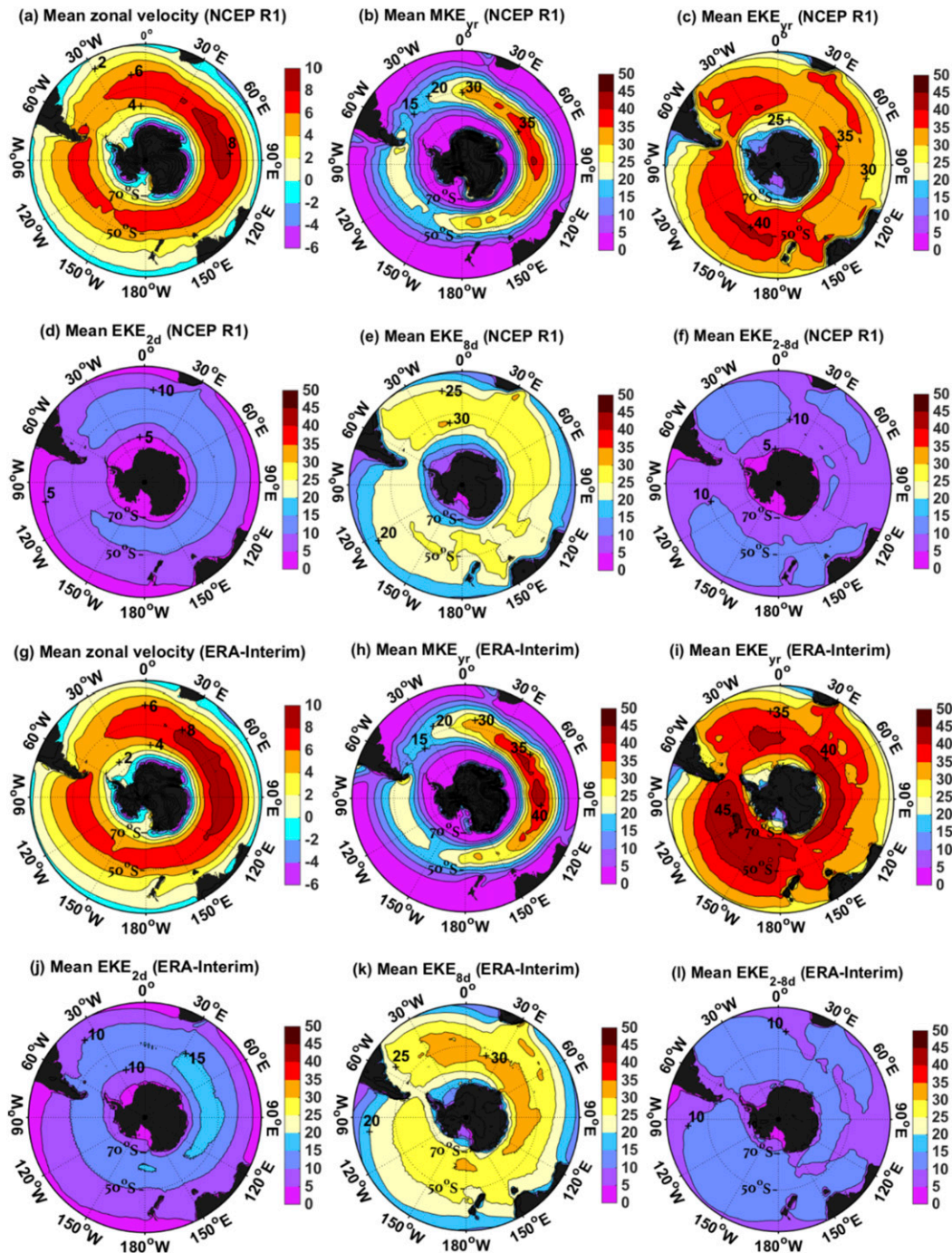


FIG. 5. The 1979–2016 time-mean zonal wind velocity ( $\text{m s}^{-1}$ ), MKE ( $\text{m}^2 \text{s}^{-2}$ ), and EKE ( $\text{m}^2 \text{s}^{-2}$ ) in the SO from (a)–(f) NCEP-1 and (g)–(l) ERA-Interim.

EKE calculated from wind fluctuations on time scales of 6 h–2 days, 2–8 days, and 6 h–8 days is found to account for about 32%, 28%, and 71%, respectively, of the total EKE for both NCEP-1 (Fig. 4b) and ERA-Interim (Fig. 4d). These EKE percentages are broadly comparable to the percentage increases of the mean stress after

including wind fluctuations on different time scales, demonstrating that the effect of wind variability on the strength of the mean stress via the nonlinear stress law depends on the magnitude of the wind variability. Stronger wind variability in ERA-Interim also contributes to the larger mean stress in ERA-Interim than



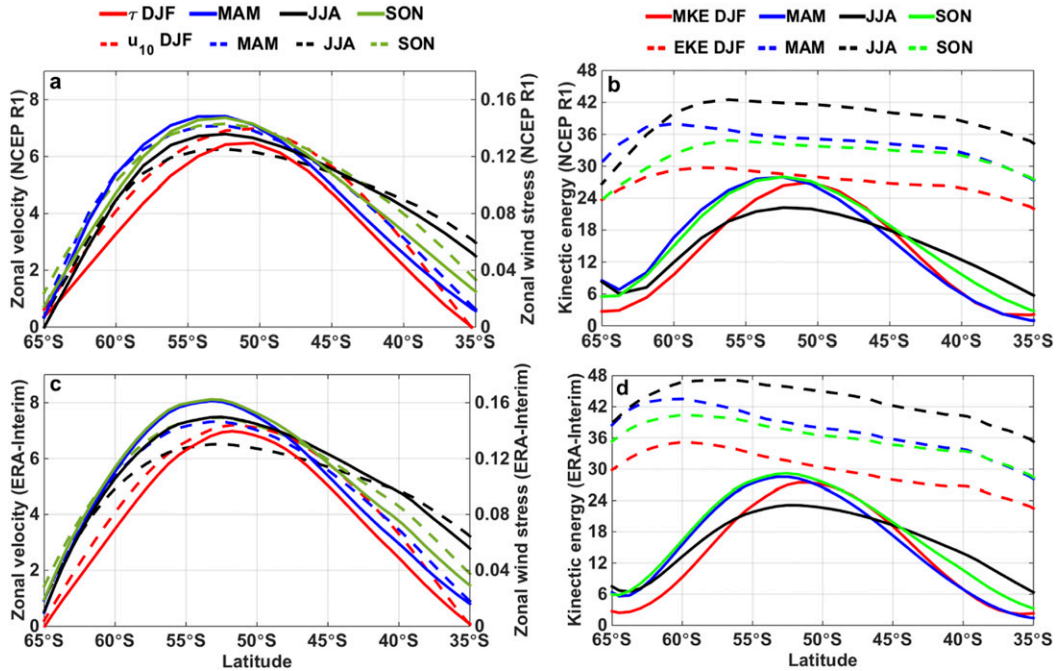


FIG. 6. The 1979–2016 zonal-mean and seasonal-mean zonal wind velocity (dashed;  $\text{m s}^{-1}$ ), zonal wind stress (solid;  $\text{N m}^{-2}$ ), MKE (solid;  $\text{m}^2 \text{s}^{-2}$ ), and EKE (dashed;  $\text{m}^2 \text{s}^{-2}$ ) from (a),(b) NCEP-1 and (c),(d) ERA-Interim.

NCEP-1 (red lines in Figs. 4a,c), although the mean winds in the two reanalysis products are comparable in strength (dashed blue).

For both reanalysis products, the zonal-mean wind peaks in austral spring and autumn (dashed green and blues lines in Figs. 6a,c), while it shifts equatorward in austral summer (dashed red) and becomes weaker but broader in austral winter (dashed black). Interestingly, the zonal-mean wind stress in austral winter (solid black) is greater than that in austral summer (solid red), even in the latitude band of  $44^{\circ}$ – $56^{\circ}\text{S}$ , where the mean wind is noticeably weaker in austral winter than in austral summer (dashed black vs dashed red). This paradox is explained by the pronounced seasonal cycle of the EKE in the SO (Figs. 6b,d), characterized by EKE being the largest in austral winter (dashed black) and smallest in austral summer (dashed red). Stronger wind variability in austral winter increases the magnitude of the mean stress much more significantly than that in austral summer, resulting in the larger mean stress seen in austral winter. It is worth pointing out that EKE is greater than MKE in the SO in all four seasons for both reanalysis products (Figs. 6b,d).

*b. Variability*

In this section, we investigate the role of wind fluctuations in determining wind stress differences between positive and negative SAM years. Here, a year

with  $\text{SAM} > 0.5$  is defined as a positive SAM year, and a year with  $\text{SAM} < -0.5$  is a negative SAM year (Fig. 7).

Figure 8 shows the mean stress,  $\text{MKE}_{\text{yr}}$ , and  $\text{EKE}_{\text{yr}}$  in positive and negative SAM years calculated from NCEP-1 (Figs. 8a–h) and ERA-Interim winds (Figs. 8i–p). Consistent with previous studies, both the mean wind and mean stress in positive SAM years (Figs. 8a,i) are found to be considerably stronger and also shifted poleward by a few degrees (Figs. 9a,b,d,e), with respect to those in negative SAM years (Figs. 8e,m). In contrast, the mean

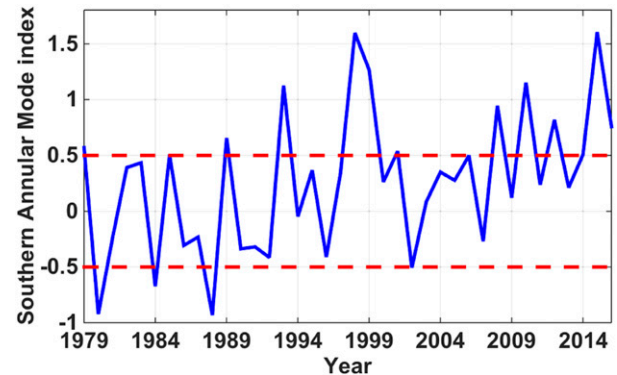


FIG. 7. The 1979–2016 station-based SAM index from Marshall (2003; updated online). Years with  $\text{SAM} > 0.5$  are defined here as positive SAM years, and those with  $\text{SAM} < -0.5$  are negative SAM years.

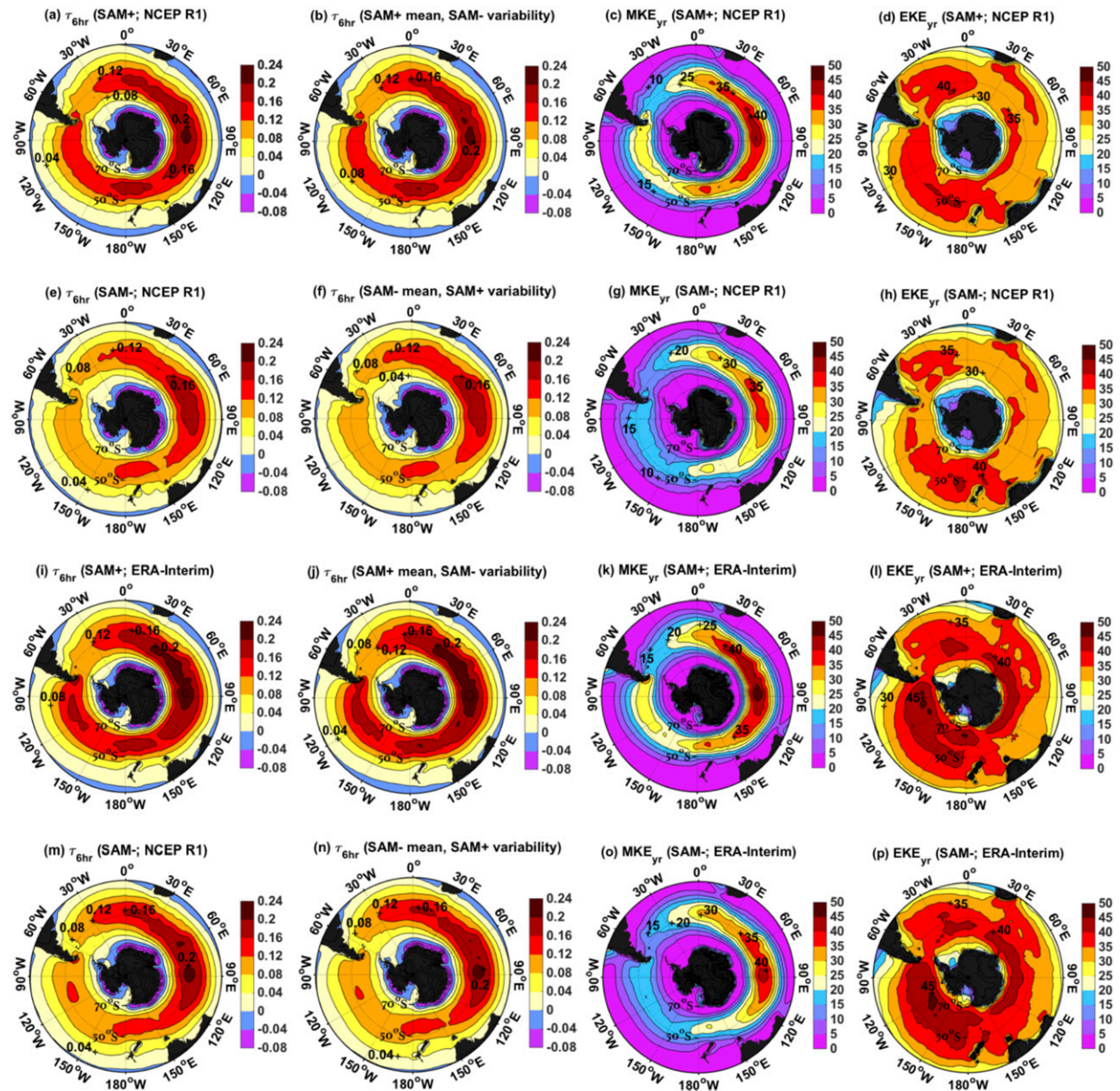


FIG. 8. The mean  $\tau_{6hr}$  ( $N m^{-2}$ ),  $MKE_{yr}$ , and  $EKE_{yr}$  ( $m^2 s^{-2}$ ) averaged over positive and negative SAM years during 1979–2016 from (a)–(h) NCEP-1 and (i)–(p) ERA-Interim. (b),(j) Mean stresses calculated using a combination of the mean wind averaged over all the positive SAM years and wind fluctuations from each negative SAM year. (f),(n) Mean stresses calculated using a combination of the mean wind averaged over all the negative SAM years and wind fluctuations from each positive SAM year.

$EKE_{yr}$  shows no statistically significant differences between positive and negative SAM years in both reanalysis products (Figs. 8d,h,i,p and 9c,f). One noticeable difference between NCEP-1 and ERA-Interim is the much larger spread of  $EKE_{yr}$  in NCEP-1 (Figs. 9c,f), indicating a stronger interannual variability of  $EKE_{yr}$  in the SO in this reanalysis product. There is a hint of a poleward shift of  $EKE_{yr}$  in positive SAM years in ERA-Interim (Fig. 9f). These results show that the SAM index

is a good indicator of the strength of the mean wind and mean stress, but not as good an indicator for the strength of wind fluctuations, at least for our analysis period of 1979–2016.

To further assess the role of wind fluctuations in determining the wind stress differences seen between positive and negative SAM years, we recalculate the mean stress using a combination of the mean wind averaged over all the positive SAM years and wind

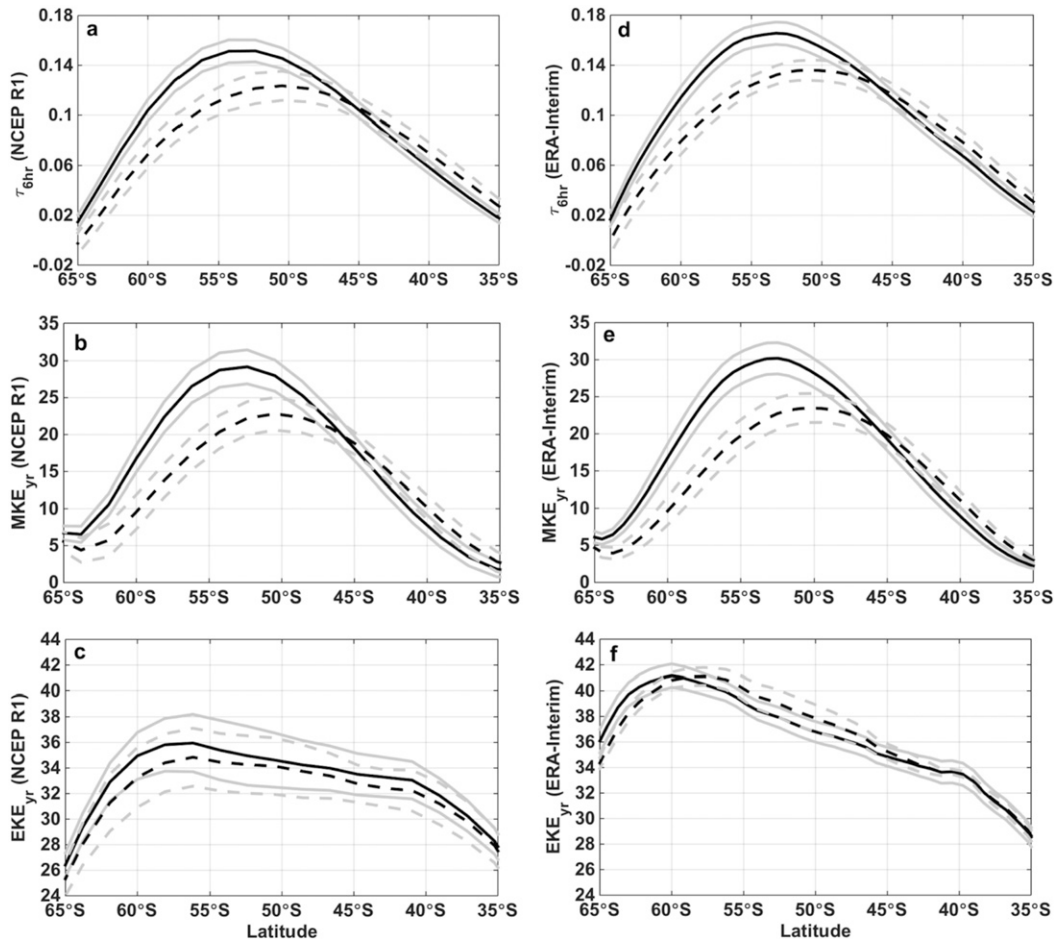


FIG. 9. (a),(d) Zonal-mean  $\tau_{6hr}$  ( $N m^{-2}$ ); (b),(e)  $MKE_{yr}$  ( $m^2 s^{-2}$ ); and (c),(f)  $EKE_{yr}$  ( $m^2 s^{-2}$ ) averaged over positive (solid black lines) and negative (dashed black lines) SAM years during 1979–2016 from (a)–(c) NCEP-1 and (d)–(f) ERA-Interim. The gray lines mark one standard deviation.

fluctuations from each negative SAM year (Figs. 8b,j), and also using a combination of the mean wind averaged over all the negative SAM years and wind fluctuations from each positive SAM year (Figs. 8f,n). Remarkably, there is virtually no difference between the mean stress in positive SAM years and the mean stress calculated using a combination of the mean wind from positive SAM years and wind fluctuations from negative SAM years (Fig. 8a vs Fig. 8b; Fig. 8i vs Fig. 8j). The same is true for the mean stress in negative SAM years and the mean stress calculated using a combination of the mean wind from negative SAM years and wind fluctuations from positive SAM years (Figs. 8e,f,m,n). This result suggests that as far as the nonlinear stress law is concerned, it is the magnitude of wind fluctuations that matters for determining the magnitude of the mean stress, not whether wind fluctuations and the mean wind are dynamically linked. The result also shows that differences in the mean wind are the key cause for the

differences in the mean stress found between positive and negative SAM years, although the presence of wind fluctuations significantly amplifies these mean stress differences; in the absence of wind fluctuations, the mean stress difference between positive and negative SAM years is much smaller (not shown). The situation in the SO appears to be in contrast to that at midlatitude North Atlantic, where stronger westerly wind stress during years of positive North Atlantic Oscillation is found to be mostly a result of enhanced synoptic wind variability, rather than a stronger background mean wind (Zhai and Wunsch 2013).

### c. Trend

We now assess the contribution of wind fluctuations to the strengthening trend of SO wind stress over the last four decades. Results from NCEP-2 and JRA-55 are also included here since they are significantly different from NCEP-1 and ERA-Interim.

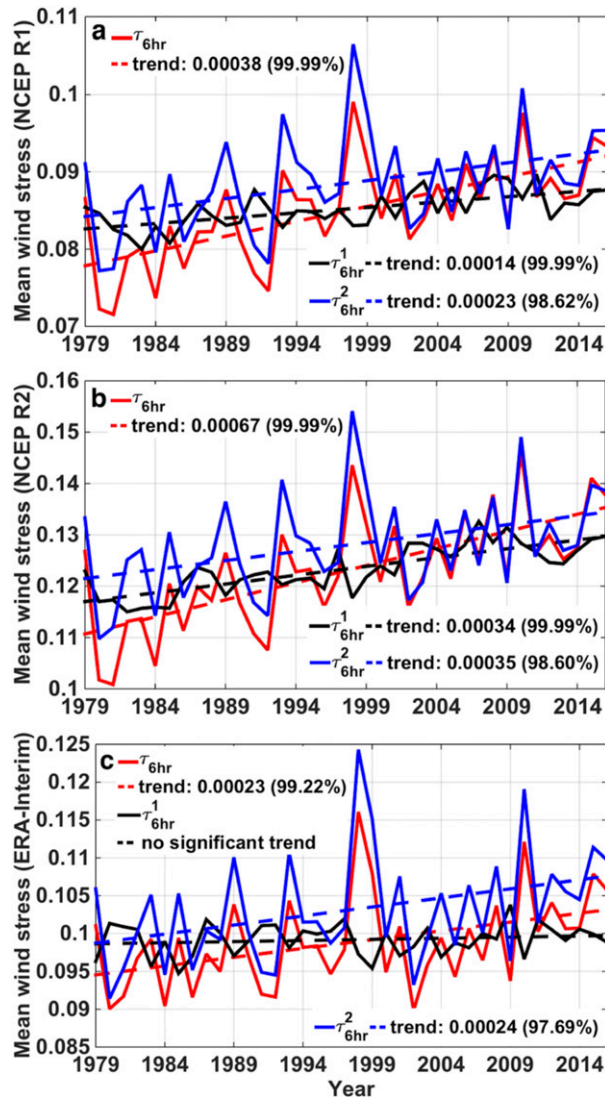


FIG. 10. Time series (red solid) and trend (red dashed) of SO wind stress averaged between 35° and 65°S during 1979–2016 from (a) NCEP-1, (b) NCEP-2, and (c) ERA-Interim. Black lines are for wind stress obtained by randomizing the annual-mean winds, and blue lines are for that obtained by randomizing wind fluctuations. Percentages in brackets show statistical significance of the trends. Note that although the overall wind stress trends are positive when averaged between 35° and 65°S, there are regions of negative trends, particularly between 35° and 45°S (not shown).

The trends of the strength of SO wind stress during 1979–2016 are  $0.00038 \text{ N m}^{-2} \text{ yr}^{-1}$  in NCEP-1 (Fig. 10a),  $0.00067 \text{ N m}^{-2} \text{ yr}^{-1}$  in NCEP-2 (Fig. 10b), and  $0.00023 \text{ N m}^{-2} \text{ yr}^{-1}$  in ERA-Interim (Fig. 10c), all significant at <1% level by *t* test, while no significant trend (<5%) is detected in JRA-55. This is consistent with the results in Thomas et al. (2015), who also found the largest trend of SO wind stress in NCEP-2 but no significant trend in JRA-55 for the period of 1980–2004.

To separate out contributions from the mean wind and wind fluctuations to the wind stress trends found in the reanalysis products, we randomly reshuffle the annual-mean wind and wind fluctuations in each year over the whole 38-yr period. First, the annual-mean wind fields are randomly reshuffled for 38 times. Each time, a new time series of wind stress is calculated using a combination of the reshuffled annual-mean wind and unshuffled wind fluctuations. We then average the 38 time series of wind stress and find the trend of the averaged stress (black lines in Fig. 10). This new trend obtained by randomizing the annual-mean winds excludes the effect of changes of the annual-mean wind and thus enables us to see how the increased intensity of wind fluctuations with time contributes to the strengthening trend of the wind stress. Similarly, we randomly reshuffle wind fluctuations of each year 38 times, calculate 38 time series of wind stress using a combination of the reshuffled wind fluctuations and unshuffled annual-mean winds, and find the trend of the time series of the averaged stress (blue lines in Fig. 10). The new trend obtained by randomizing wind fluctuations excludes the effect of changing intensity of wind fluctuations, enabling us to see how the strengthening of the annual-mean wind contributes to the strengthening trend of the wind stress.

After randomizing the annual-mean winds over the last four decades, the trends of the strength of SO wind stress are  $0.00014 \text{ N m}^{-2} \text{ yr}^{-1}$  for NCEP-1,  $0.00034 \text{ N m}^{-2} \text{ yr}^{-1}$  for NCEP-2, and  $0.00003 \text{ N m}^{-2} \text{ yr}^{-1}$  for ERA-Interim (black lines in Fig. 10). Importantly, the trends for both NCEP reanalysis products are significant at <5% level, whereas the trend for ERA-Interim is not statistically significant. Therefore, changes of wind fluctuations explain about one-third and one-half of the strengthening trend of Southern Ocean wind stress in NCEP-1 and NCEP-2, respectively, but make no significant contribution in ERA-Interim. The positive wind stress trend in ERA-Interim is due entirely to the increase in the strength of the annual-mean wind. These conclusions are supported by the calculations based on the randomization of wind fluctuations (see blue lines in Fig. 10 for the trends, as well as their statistical significance). Our study, therefore, highlights the large discrepancies among the widely used reanalysis products regarding the relative contributions of the annual-mean wind and wind fluctuations to the observed changes of SO wind stress. These discrepancies may have contributed to the diverging responses of the SO simulated by ocean models forced with different reanalysis products (Gent 2016; Munday and Zhai 2017).

Figure 11 compares the trends of  $\text{MKE}_{\text{yr}}$ ,  $\text{EKE}_{\text{yr}}$ ,  $\text{EKE}_{2\text{d}}$ ,  $\text{EKE}_{8\text{d}}$ , and  $\text{EKE}_{2-8\text{d}}$  in the three reanalysis

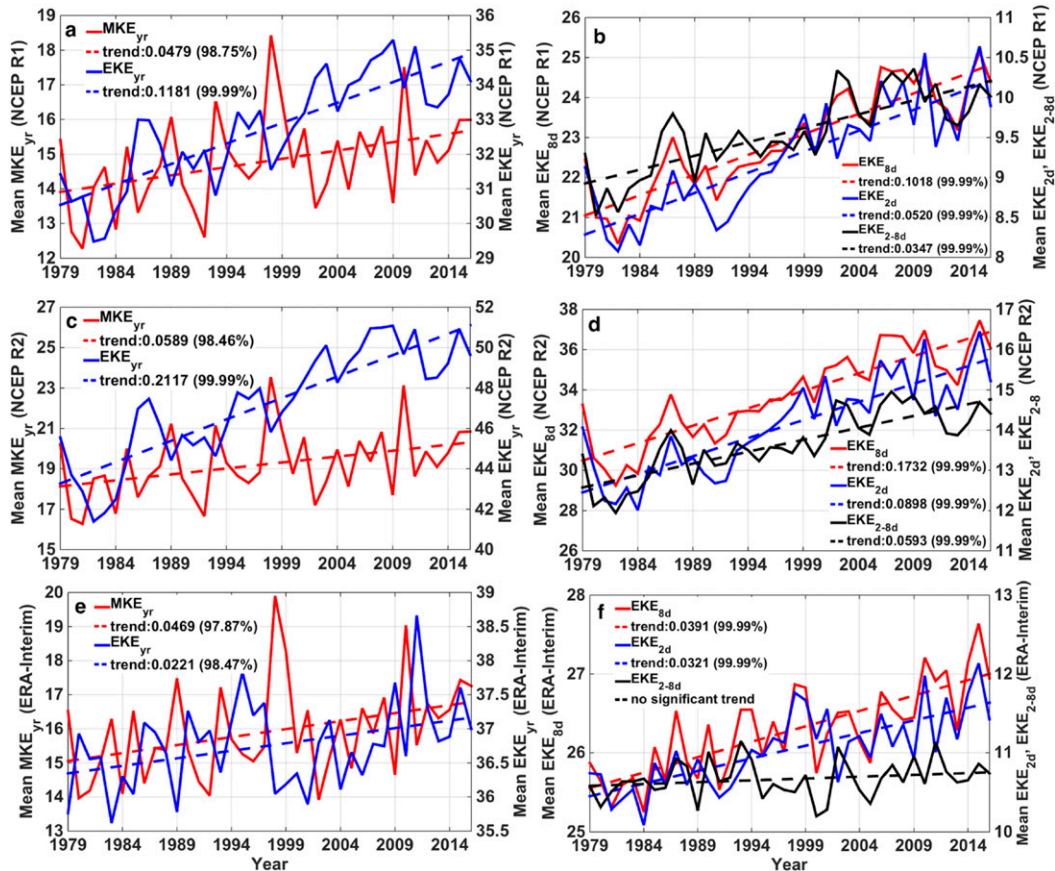


FIG. 11. Time series (solid) and trends (dashed) of  $MKE_{yr}$ ,  $EKE_{yr}$ ,  $EKE_{8d}$ ,  $EKE_{2d}$ , and  $EKE_{2-8d}$  ( $m^2 s^{-2}$ ) averaged between  $35^{\circ}$  and  $65^{\circ}$ S during 1979–2016 from (a),(b) NCEP-1; (c),(d) NCEP-2; and (e),(f) ERA-Interim. Percentages in brackets show statistical significance of the trends.

products. All the trends shown in Fig. 11 are significant at  $<5\%$  level, except for the trend of  $EKE_{2-8d}$  in ERA-Interim (black line in Fig. 11f), which is not statistically significant. The trend of  $EKE_{yr}$  in ERA-Interim (blue line in Fig. 11e), although significant, is much weaker than those in NCEP reanalysis products (blue lines in Figs. 11a,c). For example, the trends of  $EKE_{yr}$  in NCEP-1 and NCEP-2 are over 4 times and nearly 9 times greater than that in ERA-Interim, respectively. Furthermore, the trends of  $EKE_{yr}$  (blue lines) are significantly greater than the trends of  $MKE_{yr}$  (red lines) in both NCEP-1 and NCEP-2 (by 2.5 and 3.6 times, respectively; Figs. 11a,c), while the trend of  $EKE_{yr}$  is less than half of the trend of  $MKE_{yr}$  in ERA-Interim (Fig. 11e). The much weaker trend of  $EKE_{yr}$  in ERA-Interim explains why wind fluctuations make little contribution to the observed increase of SO wind stress. Over 80% of the positive trends of  $EKE_{yr}$  found in both NCEP-1 and NCEP-2 are accounted for by the trends of  $EKE_{8d}$  (red lines in Figs. 11b,d vs blue lines in Figs. 11a,c). Both  $EKE_{2d}$  and  $EKE_{2-8d}$

contribute significantly to the increase of  $EKE_{8d}$  (Figs. 11b,d). Our analysis thus shows that the SO has become stormier over the last four decades, and this increased storminess may have played an important role in the strengthening of SO wind stress, with ramifications for the sensitivity of SO stratification and circulation to wind stress changes (Munday and Zhai 2017).

The trends of the seasonal-mean SO wind stress are significant at  $<5\%$  level in all four seasons in NCEP-1, with larger trends in austral summer and autumn (Fig. 12a). In comparison, the trends of the seasonal-mean wind stress in ERA-Interim (Fig. 12c) are much smaller and only significant in austral summer and autumn. The trends of the seasonal-mean EKE in NCEP-1 (Fig. 12b) are again found to be significant in all seasons, with larger values in austral summer and autumn, while no significant trend is found in ERA-Interim in any season (Fig. 12d). These results show that wind fluctuations in NCEP-1 contribute to the strengthening of not only the annual-mean wind stress, but also the

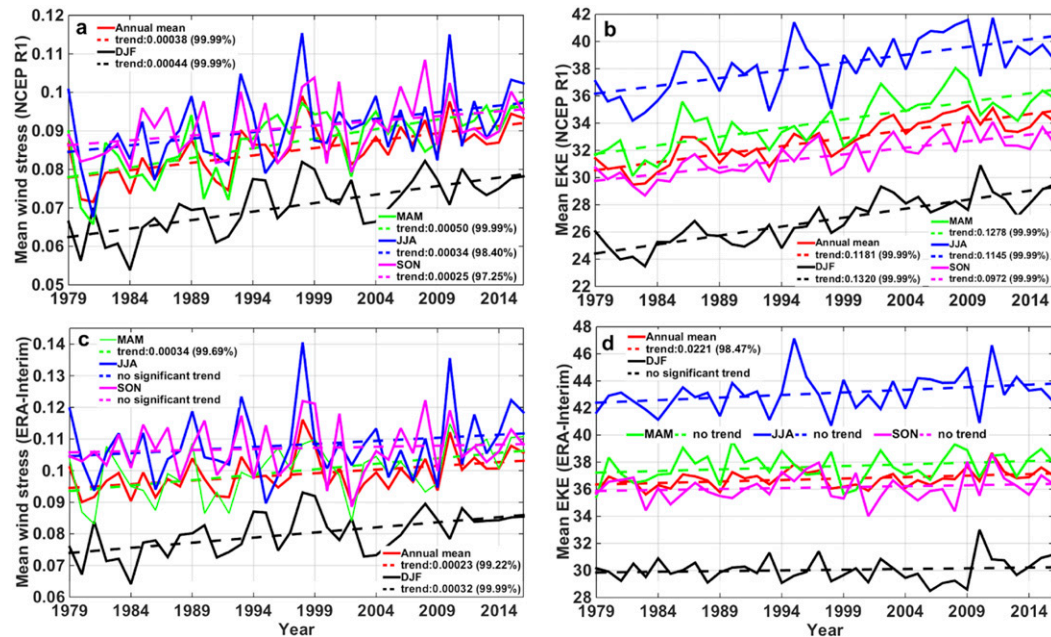


FIG. 12. Time series (solid) and trends (dashed) of the (a),(c) seasonal-mean  $\tau_{6hr}$  ( $N m^{-2}$ ) and (b),(d)  $EKE_{yr}$  ( $m^2 s^{-2}$ ) averaged between  $35^{\circ}$  and  $65^{\circ}S$  during 1979–2016 from (a),(b) NCEP-1 and (c),(d) ERA-Interim. Percentages in brackets show statistical significance of the trends.

seasonal-mean wind stress in the SO. The greater contribution to the annual-mean trend by trends in austral summer and autumn is consistent with results from previous Antarctic radiosonde data and model studies, which showed that the trend of the SH circumpolar westerly is stronger during austral summer and autumn (Thompson and Solomon 2002; Fogt et al. 2009; Jones et al. 2016), as a result of the development of the Antarctic ozone depletion during the austral summer season (Gillett and Thompson 2003; Thompson et al. 2011).

#### 4. Summary and conclusions

The Southern Ocean plays a key role in regulating the global climate via its residual meridional overturning circulation and the Antarctic Circumpolar Current. It is therefore an important task to understand how the SO responds to the observed and predicted strengthening of the westerly wind stress. Recently, Munday and Zhai (2017) showed that the sensitivity of SO stratification and circulation to wind stress changes depends strongly on whether these changes in wind stress are brought about by changes of the mean wind or wind fluctuations. However, it is yet unknown whether wind fluctuations have played a role in shaping the observed wind stress changes in the SO. In this study, we have analyzed two widely used atmospheric reanalysis products to assess the contribution of wind fluctuations to the mean,

variability, and trend of SO wind stress over the last four decades. Our main findings are as follows:

- Wind fluctuations, particularly those associated with weather systems and baroclinic storms, significantly enhance the strength of the mean wind stress in the SO. The magnitude of peak zonal-mean wind stresses is found to be doubled when wind fluctuations are included in the stress calculation. Over 70% of this doubling effect is owing to fluctuations that last less than 8 days, that is, associated primarily with weather systems/baroclinic storms.
- The SAM index is a good indicator for the mean westerly wind and wind stress, but it is not as good a measure for wind fluctuations. Both the mean wind and mean wind stress are considerably stronger and also shifted poleward (by a few degrees) during positive SAM years. In comparison, no significant differences in wind fluctuations are found between positive and negative SAM years. Therefore, stronger wind stresses during positive SAM years are due mainly to the stronger background mean winds, not enhanced wind variability, although the presence of wind fluctuations significantly amplifies wind stress differences between positive and negative SAM years.
- Large discrepancies are found among the reanalysis products analyzed in this study regarding the contribution of wind fluctuations to the strengthening trend

of SO wind stress. The intensities of wind fluctuations in NCEP-1 and NCEP-2 have increased significantly over the last four decades and are found to contribute to about one-third and one-half of the increase in the strength of SO wind stress, respectively. In contrast, the intensity of wind fluctuations only experiences a very modest increase in ERA-Interim, and as such, the wind stress trend in ERA-Interim is explained almost entirely by the strengthening of the mean westerly wind. Furthermore, the majority (over 80%) of the increase in wind fluctuations in NCEP-1 and NCEP-2 is found to be associated with weather systems and baroclinic storms. No significant trend is detected in JRA-55.

- The intensity of wind fluctuations exhibits a pronounced seasonal cycle, being highest in austral winter and lowest in austral summer. As a result, the peak zonal-mean wind stress is greater in austral winter than in austral summer, despite the mean westerly wind being stronger in austral summer than austral winter. Furthermore, trends in austral summer and autumn are found to contribute most to the annual trend in the SO.

Results from this study highlight the important contributions of wind fluctuations, especially those associated with weather systems and baroclinic storms, to the mean, variability, and trend of SO wind stress. Both NCEP reanalysis and ERA-Interim products show that the SO has become stormier over the last four decades, although the increase in atmospheric storminess is very modest in ERA-Interim. The large discrepancies found among reanalysis products regarding the contributions of wind fluctuations to the strengthening trend of SO wind stress are worrying, since not only the magnitude of the increased wind stress, but also how this increase comes about matters for the SO response to changes in wind stress forcing (Munday and Zhai 2017). The discrepancies among reanalysis products also highlight the need to have sustained observations with better coverage in the SO in order to better understand the atmospheric forcing and its changes in a region that is vital for the global climate system.

*Acknowledgments.* This study is supported by the National Key R&D Program of China (2016YFA0601804). XL is supported by a scholarship from the Chinese Scholarship Council and by the National Natural Science Foundation of China (41406214). XZ acknowledges additional support from the School of Environmental Sciences, University of East Anglia. ZW is supported by the Fundamental Research Funds for the Central Universities (2017B04814 and 2017B20714). DRM is supported by the Natural Environment Research Council (ORCHESTRA; Grant NE/N018095/1). We wish to thank Clothilde Langlais and two anonymous reviewers

for their constructive comments that led to an improved manuscript.

## REFERENCES

- Bishop, S. P., P. R. Gent, F. O. Bryan, A. F. Thompson, M. C. Long, and R. Abernathy, 2016: Southern Ocean overturning compensation in an eddy-resolving climate simulation. *J. Phys. Oceanogr.*, **46**, 1575–1592, <https://doi.org/10.1175/JPO-D-15-0177.1>.
- Böning, C. W., A. Dispert, M. Visbeck, S. R. Rintoul, and F. U. Schwarzkopf, 2008: The response of the Antarctic Circumpolar Current to recent climate change. *Nat. Geosci.*, **1**, 864–869, <https://doi.org/10.1038/ngeo362>.
- Chang, E. K. M., 2017: Projected significant increase in the number of extreme extratropical cyclones in the Southern Hemisphere. *J. Climate*, **30**, 4915–4935, <https://doi.org/10.1175/JCLI-D-16-0553.1>.
- Dee, D. P., and Coauthors, 2011: The ERA-Interim reanalysis: Configuration and performance of the data assimilation system. *Quart. J. Roy. Meteor. Soc.*, **137**, 553–597, <https://doi.org/10.1002/qj.828>.
- Downes, S. M., A. S. Budnick, J. L. Sarmiento, and R. Farneti, 2011: Impacts of wind stress on the Antarctic Circumpolar Current fronts and associated subduction. *Geophys. Res. Lett.*, **38**, L11605, <https://doi.org/10.1029/2011GL047668>.
- Dufour, C. O., J. Le Sommer, J. D. Zika, M. Gehlen, J. C. Orr, P. Mathiot, and B. Barnier, 2012: Standing and transient eddies in the response of the Southern Ocean meridional overturning to the southern annular mode. *J. Climate*, **25**, 6958–6974, <https://doi.org/10.1175/JCLI-D-11-00309.1>.
- Farneti, R., T. L. Delworth, A. J. Rosati, S. M. Griffies, and F. Zeng, 2010: The role of mesoscale eddies in the rectification of the Southern Ocean response to climate change. *J. Phys. Oceanogr.*, **40**, 1539–1557, <https://doi.org/10.1175/2010JPO4353.1>.
- Fogt, R. L., J. Perlwitz, A. Monaghan, D. Bromwich, J. Jones, and G. Marshall, 2009: Historical SAM variability. Part II: Twentieth-century variability and trends from reconstructions, observations, and the IPCC AR4 models. *J. Climate*, **22**, 5346–5365, <https://doi.org/10.1175/2009JCLI2786.1>.
- Franzke, C., T. J. O’Kane, D. Monselesan, J. Risbey, and I. Horenko, 2015: Systematic attribution of observed Southern Hemispheric circulation trends to external forcing and internal variability. *Nonlinear Processes Geophys.*, **22**, 513–525, <https://doi.org/10.5194/npg-22-513-2015>.
- Gent, P., 2016: Effects of Southern Hemisphere wind changes on the meridional overturning circulation in ocean models. *Annu. Rev. Mar. Sci.*, **8**, 79–94, <https://doi.org/10.1146/annurev-marine-122414-033929>.
- Gillett, N. P., and D. W. J. Thompson, 2003: Simulation of recent Southern Hemisphere climate change. *Science*, **302**, 273–275, <https://doi.org/10.1126/science.1087440>.
- Gong, D., and S. Wang, 1999: Definition of Antarctic oscillation index. *Geophys. Res. Lett.*, **26**, 459–462, <https://doi.org/10.1029/1999GL900003>.
- Grieger, J., G. C. Leckebusch, M. G. Donat, M. Schuster, and U. Ulbrich, 2014: Southern Hemisphere winter cyclone activity under recent and future climate conditions in multi-model AOGCM simulations. *Int. J. Climatol.*, **34**, 3400–3416, <https://doi.org/10.1002/joc.3917>.
- Hallberg, R., and A. Gnanadesikan, 2001: An exploration of the role of transient eddies in determining the transport of a zonally

- reentrant current. *J. Phys. Oceanogr.*, **31**, 3312–3330, [https://doi.org/10.1175/1520-0485\(2001\)031<3312:AEOTRO>2.0.CO;2](https://doi.org/10.1175/1520-0485(2001)031<3312:AEOTRO>2.0.CO;2).
- , and —, 2006: The role of eddies in determining the structure and response of the wind-driven Southern Hemisphere overturning: Results from the Modeling Eddies in the Southern Ocean (MESO) project. *J. Phys. Oceanogr.*, **36**, 2232–2252, <https://doi.org/10.1175/JPO2980.1>.
- Hines, K. M., D. H. Bromwich, and G. J. Marshall, 2000: Artificial surface pressure trends in the NCEP–NCAR reanalysis over the Southern Ocean and Antarctica. *J. Climate*, **13**, 3940–3952, [https://doi.org/10.1175/1520-0442\(2000\)013<3940:ASPTIT>2.0.CO;2](https://doi.org/10.1175/1520-0442(2000)013<3940:ASPTIT>2.0.CO;2).
- Hogg, A. M., P. Spence, O. A. Saenko, and S. M. Downes, 2017: The energetics of Southern Ocean upwelling. *J. Phys. Oceanogr.*, **47**, 135–153, <https://doi.org/10.1175/JPO-D-16-0176.1>.
- Inatsu, M., and B. J. Hoskins, 2004: The zonal asymmetry of the Southern Hemisphere winter storm track. *J. Climate*, **17**, 4882–4892, <https://doi.org/10.1175/JCLI-3232.1>.
- Jones, J. M., and Coauthors, 2016: Assessing recent trends in high-latitude Southern Hemisphere surface climate. *Nat. Climate Change*, **6**, 917–926, <https://doi.org/10.1038/nclimate3103>.
- Jouanno, J., X. Capet, G. Madec, G. Roullet, and P. Klein, 2016: Dissipation of the energy imparted by mid-latitude storms in the Southern Ocean. *Ocean Sci.*, **12**, 743–769, <https://doi.org/10.5194/os-12-743-2016>.
- Jung, T., S. K. Gulev, I. Rudeva, and V. Soloviev, 2006: Sensitivity of extratropical cyclone characteristics to horizontal resolution in the ECMWF model. *Quart. J. Roy. Meteor. Soc.*, **132**, 1839–1857, <https://doi.org/10.1256/qj.05.212>.
- Kalnay, E., and Coauthors, 1996: The NCEP/NCAR 40-Year Reanalysis Project. *Bull. Amer. Meteor. Soc.*, **77**, 437–471, [https://doi.org/10.1175/1520-0477\(1996\)077<0437:TNYRP>2.0.CO;2](https://doi.org/10.1175/1520-0477(1996)077<0437:TNYRP>2.0.CO;2).
- Kanamitsu, M., W. Ebisuzaki, J. Woollen, S.-K. Yang, J. J. Hnilo, M. Fiorino, and G. L. Potter, 2002: NCEP–DOE AMIP-II reanalysis (R-2). *Bull. Amer. Meteor. Soc.*, **83**, 1631–1644, <https://doi.org/10.1175/BAMS-83-11-1631>.
- Kobayashi, S., and Coauthors, 2015: The JRA-55 Reanalysis: General specifications and basic characteristics. *J. Meteor. Soc. Japan*, **93**, 5–48, <https://doi.org/10.2151/jmsj.2015-001>.
- Langlais, C., S. Rintoul, and J. Zika, 2015: Sensitivity of Antarctic Circumpolar Current transport and eddy activity to wind patterns in the Southern Ocean. *J. Phys. Oceanogr.*, **45**, 1051–1067, <https://doi.org/10.1175/JPO-D-14-0053.1>.
- Large, W. G., J. C. McWilliams, and S. C. Doney, 1994: Oceanic vertical mixing: A review and a model with a nonlocal boundary layer parameterization. *Rev. Geophys.*, **32**, 363–403, <https://doi.org/10.1029/94RG01872>.
- Le Quéré, C., and Coauthors, 2007: Saturation of the Southern Ocean CO<sub>2</sub> sink due to recent climate change. *Science*, **316**, 1735–1738, <https://doi.org/10.1126/science.1136188>.
- Marshall, G. J., 2003: Trends in the southern annular mode from observations and reanalyses. *J. Climate*, **16**, 4134–4143, [https://doi.org/10.1175/1520-0442\(2003\)016<4134:TITSAM>2.0.CO;2](https://doi.org/10.1175/1520-0442(2003)016<4134:TITSAM>2.0.CO;2).
- Marshall, J., and K. Speer, 2012: Closure of the meridional overturning circulation through Southern Ocean upwelling. *Nat. Geosci.*, **5**, 171–180, <https://doi.org/10.1038/ngeo1391>.
- Meredith, M. P., and A. M. Hogg, 2006: Circumpolar response of Southern Ocean eddy activity to a change in the southern annular mode. *Geophys. Res. Lett.*, **33**, L16608, <https://doi.org/10.1029/2006GL026499>.
- Munday, D. R., and X. Zhai, 2015: Sensitivity of Southern Ocean circulation to wind stress changes: Role of relative wind stress. *Ocean Modell.*, **95**, 15–24, <https://doi.org/10.1016/j.ocemod.2015.08.004>.
- , and —, 2017: The impact of atmospheric storminess on the sensitivity of Southern Ocean circulation to wind stress changes. *Ocean Modell.*, **115**, 14–26, <https://doi.org/10.1016/j.ocemod.2017.05.005>.
- , H. L. Johnson, and D. P. Marshall, 2013: Eddy saturation of equilibrated circumpolar currents. *J. Phys. Oceanogr.*, **43**, 507–532, <https://doi.org/10.1175/JPO-D-12-095.1>.
- O’Kane, T. J., R. J. Matear, M. A. Chamberlain, J. S. Risbey, B. M. Sloyan, and I. Horenko, 2013: Decadal variability in an OGCM Southern Ocean: Intrinsic modes, forced modes and metastable states. *Ocean Modell.*, **69**, 1–21, <https://doi.org/10.1016/j.ocemod.2013.04.009>.
- Screen, J. A., N. P. Gillett, D. P. Stevens, G. J. Marshall, and H. K. Roscoe, 2009: The role of eddies in the Southern Ocean temperature response to the southern annular mode. *J. Climate*, **22**, 806–818, <https://doi.org/10.1175/2008JCLI2416.1>.
- Simmonds, I., and K. Keay, 2000: Mean Southern Hemisphere extratropical cyclone behavior in the 40-year NCEP–NCAR reanalysis. *J. Climate*, **13**, 873–885, [https://doi.org/10.1175/1520-0442\(2000\)013<0873:MSHECB>2.0.CO;2](https://doi.org/10.1175/1520-0442(2000)013<0873:MSHECB>2.0.CO;2).
- Sinha, A., and R. P. Abernathy, 2016: Time scales of Southern Ocean eddy equilibration. *J. Phys. Oceanogr.*, **46**, 2785–2805, <https://doi.org/10.1175/JPO-D-16-0041.1>.
- Spence, P., S. M. Griffies, M. H. England, A. M. Hogg, O. A. Saenko, and N. C. Jourdain, 2014: Rapid subsurface warming and circulation changes of Antarctic coastal waters by poleward shifting winds. *Geophys. Res. Lett.*, **41**, 4601–4610, <https://doi.org/10.1002/2014GL060613>.
- Straub, D. N., 1993: On the transport and angular momentum balance of channel models of the Antarctic Circumpolar Current. *J. Phys. Oceanogr.*, **23**, 776–782, [https://doi.org/10.1175/1520-0485\(1993\)023<0776:OTTAAM>2.0.CO;2](https://doi.org/10.1175/1520-0485(1993)023<0776:OTTAAM>2.0.CO;2).
- Swart, N. C., and J. C. Fyfe, 2012: Observed and simulated changes in the Southern Hemisphere surface westerly wind-stress. *Geophys. Res. Lett.*, **39**, L16711, <https://doi.org/10.1029/2012GL052810>.
- Thomas, J. L., D. W. Waugh, and A. Gnanadesikan, 2015: Southern Hemisphere extratropical circulation: Recent trends and natural variability. *Geophys. Res. Lett.*, **42**, 5508–5515, <https://doi.org/10.1002/2015GL064521>.
- Thompson, D. W. J., and S. Solomon, 2002: Interpretation of recent Southern Hemisphere climate change. *Science*, **296**, 895–899, <https://doi.org/10.1126/science.1069270>.
- , —, P. J. Kushner, M. H. England, K. M. Grise, and D. J. Karoly, 2011: Signatures of the Antarctic ozone hole in Southern Hemisphere surface climate change. *Nat. Geosci.*, **4**, 741–749, <https://doi.org/10.1038/ngeo1296>.
- Tilina, N., S. K. Gulev, I. Rudeva, and P. Koltermann, 2013: Comparing cyclone life cycle characteristics and their interannual variability in different reanalyses. *J. Climate*, **26**, 6419–6438, <https://doi.org/10.1175/JCLI-D-12-00777.1>.
- Trenberth, K. E., 1991: Storm tracks in the Southern Hemisphere. *J. Atmos. Sci.*, **48**, 2159–2178, [https://doi.org/10.1175/1520-0469\(1991\)048<2159:STITSH>2.0.CO;2](https://doi.org/10.1175/1520-0469(1991)048<2159:STITSH>2.0.CO;2).
- Turner, J., and Coauthors, 2004: The SCAR READER Project: Toward a high-quality database of mean Antarctic meteorological observations. *J. Climate*, **17**, 2890–2898, [https://doi.org/10.1175/1520-0442\(2004\)017<2890:TSRPTA>2.0.CO;2](https://doi.org/10.1175/1520-0442(2004)017<2890:TSRPTA>2.0.CO;2).
- Verezemskaya, P., N. Tilina, S. Gulev, I. A. Renfrew, and M. Lazzara, 2017: Southern Ocean mesocyclones and polar



- lows from manually tracked satellite mosaics. *Geophys. Res. Lett.*, **44**, 7985–7993, <https://doi.org/10.1002/2017GL074053>.
- Viebahn, J., and C. Eden, 2010: Towards the impact of eddies on the response of the Southern Ocean to climate change. *Ocean Modell.*, **34**, 150–165, <https://doi.org/10.1016/j.ocemod.2010.05.005>.
- Wang, X. L., Y. Feng, R. Chan, and V. Isaac, 2016: Inter-comparison of extra-tropical cyclone activity in nine reanalysis datasets. *Atmos. Res.*, **181**, 133–153, <https://doi.org/10.1016/j.atmosres.2016.06.010>.
- Wang, Z., X. Zhang, Z. Guan, B. Sun, X. Yang, and C. Liu, 2015: An atmospheric origin of the multi-decadal bipolar seesaw. *Sci. Rep.*, **5**, 8909, <https://doi.org/10.1038/srep08909>.
- , Y. Wu, X. Lin, C. Liu, and Z. Xie, 2017: Impacts of open-ocean deep convection in the Weddell Sea on coastal and bottom water temperature. *Climate Dyn.*, **48**, 2967–2981, <https://doi.org/10.1007/s00382-016-3244-y>.
- Wu, Y., X. Zhai, and Z. Wang, 2016: Impact of synoptic atmospheric forcing on the mean ocean circulation. *J. Climate*, **29**, 5709–5724, <https://doi.org/10.1175/JCLI-D-15-0819.1>.
- , —, and —, 2017: Decadal-mean impact of including ocean surface currents in bulk formula on surface air–sea fluxes and ocean general circulation. *J. Climate*, **30**, 9511–9525, <https://doi.org/10.1175/JCLI-D-17-0001.1>.
- Yin, J. H., 2005: A consistent poleward shift of the storm tracks in simulations of 21st century climate. *Geophys. Res. Lett.*, **32**, L18701, <https://doi.org/10.1029/2005GL023684>.
- Zappa, G., L. Shaffrey, and K. I. Hodges, 2014: Can polar lows be objectively identified and tracked in the ECMWF operational analysis and the ERA-Interim reanalysis? *Mon. Wea. Rev.*, **142**, 2596–2608, <https://doi.org/10.1175/MWR-D-14-00064.1>.
- Zhai, X., 2013: On the wind mechanical forcing of the ocean general circulation. *J. Geophys. Res. Oceans*, **118**, 6561–6577, <https://doi.org/10.1002/2013JC009086>.
- , and C. Wunsch, 2013: On the variability of wind power input to the oceans with a focus on the subpolar North Atlantic. *J. Climate*, **26**, 3892–3903, <https://doi.org/10.1175/JCLI-D-12-00472.1>.
- , and D. R. Munday, 2014: Sensitivity of Southern Ocean overturning to wind stress changes: Role of surface restoring time scales. *Ocean Modell.*, **84**, 12–25, <https://doi.org/10.1016/j.ocemod.2014.09.004>.
- , H. L. Johnson, D. P. Marshall, and C. Wunsch, 2012: On the wind power input to the ocean general circulation. *J. Phys. Oceanogr.*, **42**, 1357–1365, <https://doi.org/10.1175/JPO-D-12-09.1>.
- Zhou, S., X. Zhai, and I. A. Renfrew, 2018: The impact of high-frequency weather systems on SST and surface mixed layer in the central Arabian Sea. *J. Geophys. Res. Oceans*, **123**, 1091–1104, <https://doi.org/10.1002/2017JC013609>.